

ARTICLE

Macrosystems Ecology

# Gradient surface metrics of ecosystem structural diversity and their relationship with productivity across macrosystems

Elizabeth A. LaRue<sup>1</sup>  | Kylie M. Rezendes<sup>1</sup>  | Dennis H. Choi<sup>2</sup>  |  
 Jianmin Wang<sup>2</sup>  | Anna G. Downing<sup>1</sup>  | Songlin Fei<sup>2</sup>  | Brady S. Hardiman<sup>2,3</sup> 

<sup>1</sup>Department of Biological Sciences, The University of Texas at El Paso, El Paso, Texas, USA

<sup>2</sup>Department of Forestry and Natural Resources, Purdue University, West Lafayette, Indiana, USA

<sup>3</sup>Division of Environmental and Ecological Engineering, Purdue University, West Lafayette, Indiana, USA

**Correspondence**

Elizabeth A. LaRue  
 Email: [elalarue@utep.edu](mailto:elalarue@utep.edu)

**Funding information**

GEO-Microsoft Planetary Computer Credits Programme; Directorate for Biological Sciences, Grant/Award Numbers: 1926538, 2106103, 2212859; National Institute of Food and Agriculture, Grant/Award Numbers: 2023-68012-38992, 2024-67021-42879

**Handling Editor:** Kristofer D. Johnson

## Abstract

Structural diversity—the volume and physical arrangement of vegetation within the three-dimensional (3D) space of ecosystems—is a predictor of ecosystem function that can be measured at large scales with remote sensing. However, the landscape composition and configuration of structural diversity across macrosystems have not been well described. Using a relatively recently developed method to quantify landscape composition and configuration of continuous habitat or terrain, we propose the application of gradient surface metrics (GSMs) to quantify landscape patterns of structural diversity and provide insights into how its spatial pattern relates to ecosystem function. We first applied an example set of GSMs that represent landscape heterogeneity, dominance, and edge density to Lidar-derived structural diversity within 28 forested landscapes at National Ecological Observatory Network (NEON) sites. Second, we tested for forest type, geographic location, and climate drivers of macro-scale variation in GSMs of structural diversity (GSM-SD). Third, we demonstrated the utility of these metrics for understanding spatial patterns of ecosystem function in a case study with NDVI, a proxy of productivity. We found that GSM-SD varied in landscapes within macrosystems, with forest type, geographic location, and climate being significantly related to some but not all metrics. We also found that dominance of high peaks of height and vertical complexity of canopy vegetation and the heterogeneity of the vertical complexity and coefficient of variation of canopy vegetation height within 120-m patches were negatively correlated with NDVI across the 28 NEON sites. However, forest type always had a significant interaction term between these GSM-SD and NDVI relationships. Our study demonstrates that GSMs are useful to describe the landscape composition and configuration of structural diversity and its relationship with productivity that warrants further consideration for spatially motivated management decisions.

This is an open access article under the terms of the [Creative Commons Attribution License](#), which permits use, distribution and reproduction in any medium, provided the original work is properly cited.

© 2025 The Author(s). *Ecosphere* published by Wiley Periodicals LLC on behalf of The Ecological Society of America.

## KEY WORDS

landscape heterogeneity, landscape structure, Lidar, National Ecological Observatory Network, vegetation structure

## INTRODUCTION

Spatial variability is an inherent part of the study of the ecological patterns and processes in nature (Guo et al., 2023; Turner & Gardner, 2015). The characterization of the landscape composition and configuration of biological diversity across macrosystems is therefore a critical part of the understanding of the interplay between ecological pattern and process (Fei et al., 2016; Gaston et al., 1995; Tscharntke et al., 2012). For instance, biogeographers have long been fascinated by the poleward decrease in species richness and its associated eco-evolutionary causes and consequences (Brodie & Mannion, 2023; Hawkins et al., 2003). With advances in technology for measuring new aspects of biological diversity beyond the traditional species richness, the landscape composition and configuration of diversity need to be quantified to better understand its underlying mechanisms and their consequences for ecosystem function (LaRue, Fahey, et al., 2023).

Three-dimensional (3D) structural diversity—the volumetric capacity and physical arrangement of the biotic components in ecosystems—is an understudied type of diversity that has the potential to be a useful tool for predicting ecosystem function across space (LaRue, Fahey, et al., 2023). Metrics of structural diversity that have been commonly described in the literature, such as the vertical stratification or heterogeneity of vegetation height within a forest stand or plot, can be easily measured with remote sensing techniques like Lidar (Ogunjemiyo et al., 2005; Zimble et al., 2003). Structural diversity has been found to be a strong predictor of ecosystem functions such as forest productivity when quantified in stands or plots (Gough et al., 2019; Hardiman et al., 2011; LaRue, Knott, et al., 2023) and thereby can be used as a tool to understand ecosystem function.

The composition and configuration of landscapes varies significantly due to climate, regional species composition, and disturbance (Turner, 1990, 2010; Turner & Gardner, 2015), which is anticipated to be reflected in the spatial variation of structural diversity within landscapes and across macrosystems as well (Dodonov & Harper, 2022; Kane et al., 2011). Despite early ecological origins (MacArthur & MacArthur, 1961), structural diversity has not been widely measured at landscape scales yet. Therefore, structural diversity's application in describing its landscape composition and configuration

patterns across macrosystems is even more limited despite the availability of new remote-sensing tools (Atkins et al., 2023; LaRue, Fahey, et al., 2023). Meanwhile, its spatial patterns from within landscapes and across macrosystems that vary in environmental conditions could be quite important in regional management applications (LaRue, Fahey, et al., 2023).

Landscape ecology has a long tradition in using patch mosaic metrics to describe discrete landscape composition and configuration patterns of land cover, but previous work had not focused on continuous spatial heterogeneity until recently (McGarigal & Dushman, 2005). Patch metrics that describe the landscape composition and configuration of categorical variables, such as land use and land cover, have been used for decades (i.e., Fragstats, McGarigal & Marks, 1995). However, equivalent metrics for continuous variables were not introduced until McGarigal et al. (2009) proposed gradient surface metrics (GSMs) as a comparable way to measure the gradient aspects of spatial composition and configuration of continuous raster values. McGarigal et al. (2009) described a suite of GSMs that clustered into four groups of similarly behaved metrics describing surface roughness, the shape of the surface height distribution, and angular and radial surface texture of continuous variables. GSMs, especially those in the surface roughness group, are correlated with many traditional patch mosaic metrics (McGarigal et al., 2009). Surface roughness GSMs are conceptually analogous to (1) overall surface spatial variability, such as nonspatially explicit composition measures of patch diversity and dominance and (2) local variability in height (slope or steepness of the surface) such as spatially explicit configuration metrics of edge density or contrast. A second group of nonspatially explicit GSMs describe the shape of the surface height distribution comparable to measures of landscape dominance and evenness, whereas the angular and radial surface texture groups of GSMs do not have readily analogous patch mosaic metrics, nor are they strongly correlated with them (McGarigal et al., 2009). In landscape ecology, GSMs have been applied to continuous variables such as elevation (Anderson et al., 2015; Read et al., 2020), vegetation indices (Smith et al., 2021), or developed city environments (Kedron et al., 2019) and may provide additional novel linkages between 3D ecological spatial patterns of diversity and process.

The previous successful applications of GSMS for viewing landscapes as a 3D environmental surface (McGarigal et al., 2009) led us to believe that GSMS would also be valuable for quantifying structural diversity at the landscape level. More specifically, GSMS can be used to summarize the equivalent of patch-level composition and configuration landscape patterns of structural diversity across local raster cells (e.g., to describe composition and configuration of  $30 \times 30$  m structural diversity cells across  $120 \times 120$  m or any size unit of patches across a landscape, e.g., Figure 1). Structural diversity in earlier work has been typically described as a value of vertical heterogeneity or height stratification at the stand or plot level and has been shown to be positively correlated with forest productivity (Aponte et al., 2020; Gough et al., 2019; Hardiman et al., 2011). However, the landscape composition and configuration (i.e., horizontal spatial patterns across smaller localized areas of structural diversity cells) might result in spatial patterns in structural diversity that will interact with ecosystem functions in ways that have not been previously explored. Hence, GSMS could provide a useful approach to quantify the composition and configuration of structural diversity metrics within landscapes and provide unique insights into how landscape patterns of structural diversity relate

to ecosystem functions. For instance, we would expect that a GSM representing the heterogeneity (spatial composition) of structural diversity within an area would have a negative relationship with ecosystem productivity, because a higher horizontal spatial variation in structural diversity will lead to a reduction in productivity due to lower functional niche space filled over the patch (LaRue, Knott, et al., 2023). Additionally, we could expect that a measure of dominance of high structural diversity peaks within an area would also have a negative relationship with productivity (Torresan et al., 2020; Zhang et al., 2024), because a dominance of many peaks of structural diversity values may cause a decrease in productivity from lower functional niche space filled (LaRue, Knott, et al., 2023). Furthermore, a spatially explicit measure of edge density of structural diversity might have a negative relationship with productivity, because high horizontal spatial variation in structural aspects of the forest within a patch will lead to lower filled niche space (LaRue, Knott, et al., 2023) or edge effects from a successional/ecotone transition that breaks up the forest canopy and reduces resource uptake (Chaplin-Kramer et al., 2015; Fahey et al., 2019; Ordway & Asner, 2020).

In this study, we are proposing a new set of measures, GSMS of structural diversity (GSM-SD), that have a

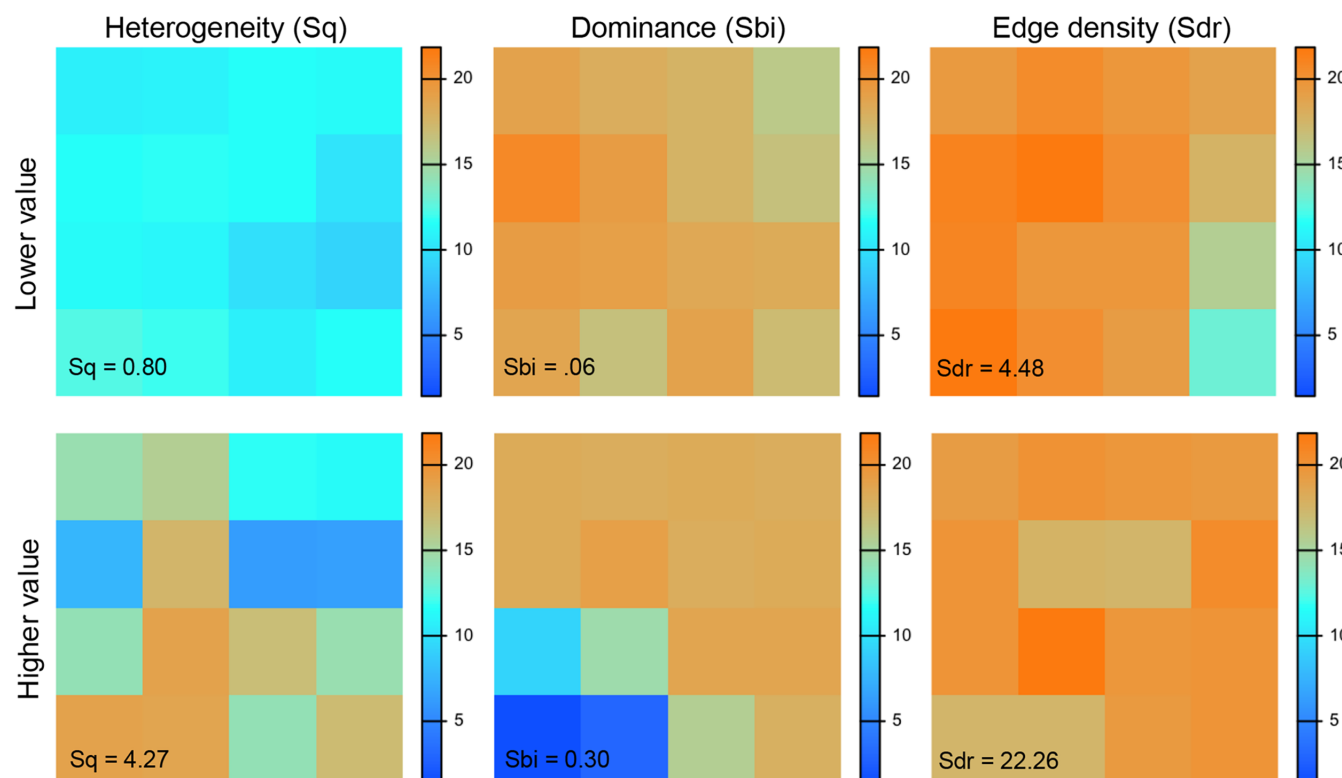


**FIGURE 1** Representative raster grids of mean canopy height within  $120 \times 120$  m patches for the NEON site BART that had low (top row) and high values (bottom row) of the three gradient surface metrics (GSMS) used in our study dataset. Metric definitions for GSMS can be found in Table 1.

**TABLE 1** GSM-SD that measure the landscape composition and configuration of structural diversity raster data.

GSM category from McGarigal et al. (2009)		Metric	Definition	Formula	Application to landscape patterns of structural diversity	Hypothesized relationship with productivity
Composition: Heterogeneity	Roughness	Root mean-square roughness (Sq)	The SD of surface values.	$Sq = \sqrt{\frac{1}{N-1} \times \sum_{i=1}^N (z_i - \bar{z})^2}$	Heterogeneity or surface roughness in the structural diversity within a patch.	Negative relationship–higher spatial variation in structural diversity will lead to a reduction in productivity due to lower functional niche space filled.
Composition: Dominance	Distribution	Surface bearing index (Sbi)	The ratio of root mean square roughness to height of the highest 5% values in the surface bearing curve.	$Sbi = \frac{Sq}{Z_{0.05}}$	A measure of the shape of the surface height profile of the structural diversity within a patch or also described as the distribution of high peaks in the surface profile. A surface with few high peaks (more even distribution) has a low value and a surface with many high peaks or no peaks has a high value.	Negative relationship—dominance of high peaks in structural diversity may cause a decrease in productivity due to lower functional niche space filled.
Configuration: Edge density	Roughness	Surface area ratio (Sdr)	Ratio of a flat surface to the actual surface.	$Sdr = \frac{\left( \sum_{k=0}^{M-2} \sum_{l=0}^{N-2} A_{kl} \right) - (M-1) \times (N-1) \delta x \delta y}{(M-1) \times (N-1) \delta x \delta y} \times 100\%$ where $A_{kl} = \frac{1}{4} \times \left( \sqrt{\delta y^2 + (z(x_k, y_l) - z(x_k, y_{l+1}))^2} + \sqrt{\delta y^2 + (z(x_{k+1}, y_l) - z(x_{k+1}, y_{l+1}))^2} + \sqrt{\delta x^2 + (z(x_k, y_l) - z(x_k+1, y_l))^2} + \sqrt{\delta x^2 + (z(x_k, y_l) - z(x_k+1, y_{l+1}))^2} \right)$	The ratio between the surface area of structural diversity values to a flat plane with the same dimensions in a patch. A low value indicates a flat surface, whereas a higher value indicates an increasing local slope or variability (increasing edge density).	Negative relationship–high spatial variation leading to lower filled niche space or a transition in succession or ecotone that results in decreased productivity.

*Note:* The definitions and formulas are from McGarigal et al. (2009) and calculated with the *geodiv R* package (Smith et al., 2021).

conceptual parallel to classic landscape ecology measures from the patch mosaic paradigm (e.g., heterogeneity, dominance, and edge density; Table 1) and demonstrate their usefulness by looking at GSM-SD correlations with ecosystem function (productivity). To do this, we addressed three objectives:

1. Generate GSM-SD to describe the landscape patterns of structural diversity from within a set of 28 different forested landscapes (i.e., sites across a macrosystem) from the National Ecological Observatory Network (NEON).
2. Investigate how forest type, geographic location, and climate are related to GSM-SD to take the first step to understand potential common macroscale drivers of their spatial patterns, because structural diversity has been shown to vary by macroscale factors such as climate (Ehbrecht et al., 2021; LaRue, Knott, et al., 2023) or ecosystem and forest type (Atkins et al., 2022; Crockett et al., 2023).
3. Demonstrate the usefulness of GSM-SD by looking at its correlation with ecosystem function with a case study—forest productivity across our macrosystems dataset. To do this, we tested if GSM-SD are correlated with NDVI from Landsat 8 as a proxy of productivity. We anticipated that greater heterogeneity, a dominance of high peaks, and edge density observed in the vertical structural diversity values within a horizontal area (i.e., as measured by GSM-SD) will be associated with a decrease in ecosystem productivity due to reduced niche space filling across the corresponding horizontal area (see Table 1 for a summary of the GSMS and their hypothesized relationships with productivity).

## MATERIALS AND METHODS

### Overview of study design

To address our study objectives, we first used Lidar for measuring structural diversity from 28 forested NEON sites that spanned 16 ecoclimatic domains in the USA (Table 2; Appendix S1: Figure S1). We then generated three GSM by four structural diversity metric combinations (i.e., 12 GSM-SD) in 50 locations with forest cover at two patch spatial grains (60 × 60 m and 120 × 120 m) within each of the 28 NEON sites. We refer to the spatial extent of each NEON site as a landscape (Appendix S1: Figure S2) and the entire collection of landscapes as a macrosystem (i.e., macroscale) for the spatial extent of the whole study system (Appendix S1: Figure S1). From each NEON site (landscape), we obtained climatic, forest

type, and geographic location information, to test for macroscale predictors of GSM-SD. Finally, we tested for linear relationships between GSM-SD and productivity (NDVI as a proxy) within individual sites and across the macrosystem (with forest type and geographic location as site-level covariates).

### Structural diversity from NEON aerial Lidar

We used a previously published structural diversity data product (Wang et al., 2023, 2024) derived from the NEON Airborne Observation Platform (AOP) level 1 Lidar (Product No. DP1.30003.001, NEON, 2025). Detailed methods can be found in Wang et al. (2024), but we provide an overview of the how structural diversity data were processed in this data product. We focused primarily on years of Lidar data that were predominantly collected using the Optech Gemini payload (first generation of Lidar payloads at NEON) to facilitate standardizing the sensor used and that were collected during peak growing season between 2017 and 2021 across the sites (Table 2). The methods for structural diversity metrics generated from the NEON AOP Lidar, included utilizing all the Lidar tiles (extent of each tile: 1 × 1 km<sup>2</sup>) within each site (wall-to-wall process within each site boundary) (Table 2; Appendix S1: Figure S1) (Wang et al., 2023, 2024). Noise points were filtered out whose heights are greater than six standard deviations from the mean height and lower than ground points. Then, 50-m buffers were set around each tile to alleviate the edge effect when normalizing the ground height to remove topographic height variation. Vegetation height was normalized using a digital terrain model interpolated through the k-nearest neighbor approach with inverse-distance weighting with the *normalize\_height* function (Roussel et al., 2020). After height normalization, the points below a height of 0.5 m were filtered out for calculating Lidar-derived metrics. All Lidar data processing and analysis were performed using the *lidR* R package (Roussel et al., 2020).

We focused on a selection of four structural diversity metrics to be used in the generation of the GSM-SD metrics. The four structural diversity metrics that we used describe different aspects of the height and interior (vertical canopy strata) complexity of vegetation—CHM, Q25, VCI, and CV(ht) (Table 3). Each site boundary had been gridded into 30 × 30 m (Wang et al., 2023), aligning both locations and UTM projections of the grids with those of Landsat 8 collections (U.S. Geological Survey, 2023). The structural diversity metrics were calculated from Lidar points within the grid across sites.

**TABLE 2** Characteristics of NEON sites and Airborne Observation Platform (AOP) Lidar data used in this study.

Forest type	Site	Ecoclimatic domain	Total annual precipitation (mm)	Mean annual temperature (°C)	AOP year	AOP area km <sup>2</sup>
Deciduous	SERC	D02	1075	13.6	2019	139
	UKFS	D06	990	12.7	2019	170
	MLBS	D07	1227	8.8	2017	143
	LENO	D08	1386	18.1	2018	155
	CLBJ	D11	926	17.5	2017	159
Evergreen	DSNY	D03	1216	22.5	2019	214
	OSBS	D03	1302	20.9	2018	227
	GUAN	D04	840	23	2018	162
	GUIL	D04	1168	25	2018	33
	DELA	D08	1372	17.6	2019	132
	RMNP	D10	731	2.9	2018	210
	YELL	D12	493	3.4	2019	284
	NIWO	D13	1005	0.3	2020	165
	ABBY	D16	2451	10	2017	166
	WREF	D16	2225	9.2	2017	251
	SOAP	D17	900	13.4	2019	198
	TEAK	D17	1223	8	2019	211
Mixed evergreen deciduous	DEJU	D19	305	-3	2019	242
	PUUM	D20	2657	12.7	2020	324
	BART	D01	1325	6.2	2019	135
	HARV	D01	1199	7.4	2019	347
	SCBI	D02	1126	11.6	2017	128
	JERC	D03	1308	19.2	2018	358
	CHEQ	D05	797	4.8	2017	65
	STEI	D05	797	4.8	2017	182
	UNDE	D05	802	4.3	2017	182
	GRSM	D07	1375	13.1	2021	271
	TALL	D08	1383	17.2	2018	177

*Note:* A random sample of 50 locations were taken from each site for a total of 1400 across 28 NEON sites.

**TABLE 3** Overview of structural diversity metrics from Lidar.

Metric	Name (unit)	Description	Reference
CHM	Mean value of canopy height model (m)	CHM is the mean of maximum height (m) in individual 1-m <sup>2</sup> grids within each 30 × 30 m <sup>2</sup> grid.	Atkins et al. (2018)
Q25	25th canopy height quantile (m)	Q25 is the 25th quantile of the Lidar points in each 30 × 30 m <sup>2</sup> grid was used as a measure of subcanopy density.	Roussel et al. (2020)
CV(ht)	Coefficient of variation of the height (unitless)	The coefficient of variation of vegetation heights, CV(ht), of the points in 30 × 30 m <sup>2</sup> grids was used as a measure of internal canopy vegetation height heterogeneity.	Roussel et al. (2020)
VCI	Vertical complexity index (unitless)	Vertical complexity index (VCI) is the normalization of diversity and evenness (entropy) of 1-m height bins within the plot to measure the diversity of stratified vegetation layers in the canopy.	van Ewijk et al. (2011)

We downloaded the four structural diversity metrics as a landscape raster mosaic for each NEON site from the Environmental Date Initiative website (Wang et al., 2023). We conducted post-processing on the structural diversity raster landscapes by masking out non-forest raster cells within each NEON site on a Microsoft Azure Data Science Microsoft Virtual Machine. The landscape that makes up each NEON site is composed of a variety of land cover types, but we focused solely on forest land cover that the structural diversity metrics were previously developed for. Therefore, the *terra* R package (Hijmans, 2024) was used to exclude non-forest landcover from our raster maps of structural diversity with a 2019 global ESRI land cover data product (ESRI Living Atlas, 2019).

## GSM-SD

GSM-SD were generated from structural diversity rasters from two sampling grids— $60 \times 60$  m and  $120 \times 120$  m—to quantifying the landscape composition and configuration of structural diversity from within 28 NEON forested sites. We selected three GSMS that have a conceptual analog to patch mosaic metrics (Table 1, also see McGarigal et al., 2009) to demonstrate their potential utility in understanding GSM-SD patterns and correlation with ecosystem function. However, there is a larger suite of GSMS interested users can access (McGarigal et al., 2009) than we could cover in the scope of this study. We used functions from the *geodiv* R package (Smith et al., 2021) to calculate three GSMS that describe heterogeneity (sq), dominance (sbi), and edge density (sdr) (Table 1) of structural diversity within  $60 \times 60$  m and  $120 \times 120$  m square areas or patches (see Figure 1 for example low and high values of  $120 \times 120$  patches for GSM-SDs). We selected a 60 and 120-m cell size, because Landsat data are provided in  $30 \times 30$  m cell sizes, and this provides multiples of two and four times the sampling grids, respectively, from our base data spatial grain. First, we randomly generated coordinates representing different locations within the landscape of each NEON site. A 0.5-km buffer around the edges of each site was included prior to randomly sampling coordinates to avoid taking patches right at the edge of the landscape. These randomly selected points were then used to create  $60 \times 60$  m and  $120 \times 120$  m square raster clips (patch) for which the respective GSM-SD were then generated from *geodiv* functions. We retained 50 patches per site that had an average outer canopy height of 3 m or greater and that did not overlap within another  $120 \times 120$  m patch for a total of 1400 patches for the entire macrosystem. The site-level distribution of values for each GSM-SD can be observed in Appendix S1: Figures S3–S5.

## NDVI as a proxy of productivity

We used NDVI as a proxy of productivity (Myneni et al., 1995; Pettorelli et al., 2005) to examine its relationship with GSM-SD across macrosystems. We downloaded Landsat 8 Collection 2-Level 2 data (U.S. Geological Survey., 2023) from the USGS Earth Explorer for calculating NDVI at spatially overlapping locations for each of the 28 NEON sites. We selected the Landsat image that had the lowest cloud cover and was collected within a couple of months of the AOP Lidar. The red and near infrared bands were used in the calculation of NDVI across the landscape from  $(\text{NIR} - \text{Red})/(\text{NIR} + \text{Red})$ . We employed a cloud cover mask using the QA\_PIXEL band provided with the Level 2 data to remove pixels with a high confidence of cloud cover. Finally, we employed the same non-forest landcover mask with the 2019 global ESRI 10-m resolution land cover data product (ESRI Living Atlas, 2019) to the NDVI raster as was done to structural diversity using the *raster* (Hijmans & van Etten, 2022) and *rgdal* R packages (Biband et al., 2022). Finally, we extracted the mean of NDVI across the cells in the same  $120 \times 120$  m and  $60 \times 60$  m patch areas that were used for GSM-SD.

## Analyses

We first calculated Spearman correlation coefficients between all GSM-SD to examine the strength of the linear relationships between them. Metrics from the 60- and 120-m patch sizes were often positively correlated (Appendix S1: Figure S6), so we conducted analyses with the 120-m patch size to avoid redundancy in our analysis output.

We tested for differences in GSM-SD by forest type, geographic location, and climate using simple linear models. A site-level forest type, latitude, longitude, total annual precipitation (in millimeters), and mean annual temperature (in degrees Celsius) values for each of the 28 sites were obtained from NEON (see Table 2). Forest type, latitude, longitude, precipitation, and temperature were tested individually as a univariate predictor of each GSM-SD to understand their individual linear relationships. GSM-SD were natural  $\log(x + 1)$  transformed to test for linear relationships, and all variables were standardized (zero mean and unit variance) to assess effect sizes after the same transformation. Negative values were removed from longitude prior to transformation and standardization. A chi-square test statistic for each coefficient was assessed at a significance level of alpha  $<0.05$  in addition to a 95% bootstrapped CI of the coefficient to examine the magnitude and direction of the slope.

We used general linear models to test if individual GSM-SD increase or decrease with NDVI. The GSM-SD,

forest type, the  $\text{GSM-SD} \times \text{forest type}$  interaction, latitude, and longitude were included as fixed effects in the model. A separate model was run for each  $\text{GSM-SD}$  ( $N_{\text{Models}} = 12$  of three  $\text{GSMs}$  by four structural diversity metric combinations).  $\text{NDVI}$  and  $\text{GSM-SD}$  were natural  $\log(x + 1)$  transformed to test for linear relationships, because previous work has shown that structural diversity and productivity relationships can be linear or hump-shaped (LaRue, Knott, et al., 2023). All variables were standardized (zero mean and unit variance) to assess effect sizes after the transformation. A chi-square test statistic for each coefficient was assessed at a significance level of alpha  $<0.05$ . To visualize the direction and magnitude of the overall macrosystems relationship between  $\text{GSM-SD}$  and  $\text{NDVI}$ , we obtained a 95% bootstrapped CI. We followed this up by site-level simple linear regressions between all pairwise combinations of  $\text{GSM-SD}$  as a correlate of  $\text{NDVI}$ . Significance of the linear slope was assessed with a 95% bootstrapped CI (if interval was not overlapping with zero).

## RESULTS

### Macrosystems patterns of variation in and drivers of $\text{GSM-SD}$

We observed both positive and negative correlations among the  $\text{GSM-SD}$  quantified across 28 NEON sites. We saw moderate to strong positive correlations between heterogeneity of structural diversity within a patch (heterogeneity  $\text{GSM-SD}$ ) and dominance of the structural diversity patch profile (dominance  $\text{GSM-SD}$ ) (Appendix S1: Figure S6), whereas the greater density of edges in structural diversity within a patch (edge density  $\text{GSM-SD}$ ) were weakly to moderately negatively correlated with the heterogeneity and dominance  $\text{GSM-SD}$  (Appendix S1: Figure S6). This indicates that these  $\text{GSM-SD}$  were describing different patterns of landscape composition and configuration of structural diversity across macrosystems.

Geographic location, forest type, and climate were significantly associated with several  $\text{GSM-SD}$ . The heterogeneity and dominance  $\text{GSM-SD}$ , except for  $\text{VCI}$ , were significantly different among forest types (Table 4, Figure 2). We also saw substantial variation in the distribution of the  $\text{GSM-SD}$  values across individual sites (Appendix S1: Figures S3–S5). The heterogeneity of  $\text{CHM}$ ,  $\text{Q25}$ , and  $\text{CV(ht)}$  and dominance of  $\text{CV(ht)}$  increased with latitude (Table 4). The heterogeneity of  $\text{CHM}$  decreased with longitude (increased to east), but the dominance and edge density of  $\text{CHM}$  increased with longitude (increased to west), and the heterogeneity of  $\text{Q25}$  and dominance of

$\text{CV(ht)}$  decreased with longitude (increased to east) (Table 4). All  $\text{GSM-SD}$  pertaining to  $\text{CHM}$  and  $\text{Q25}$  and the heterogeneity and dominance of  $\text{CV(ht)}$  increased with mean annual temperature (Table 4). The heterogeneity and edge density of  $\text{CHM}$  and  $\text{Q25}$  increased with precipitation but the dominance of  $\text{CHM}$  decreased with precipitation (Table 4). The dominance of  $\text{VCI}$  decreased with precipitation and was the only correlate of macro-scale variation in  $\text{GSMs}$  of  $\text{VCI}$  (Table 4).

### $\text{GSM-SD}$ versus forest productivity across macrosystems

Several  $\text{GSM-SD}$  that describe the heterogeneity and dominance of structural diversity within patches, but not edge density, were negatively related to  $\text{NDVI}$  across macrosystems (Table 5). The heterogeneity of  $\text{VCI}$  and  $\text{CV(ht)}$  had a significant negative relationship with  $\text{NDVI}$ . There was also an overall negative correlation between the dominance of  $\text{CHM}$ ,  $\text{Q25}$ , and  $\text{VCI}$  with  $\text{NDVI}$ . There was always a significant interaction between the dominance or heterogeneity of the four structural diversity metrics and forest type with  $\text{NDVI}$  (Table 5, Figure 3). Forest type and longitude were the strongest significantly correlated variables with  $\text{NDVI}$ , respectively, across all  $\text{GSM-SD}$ . However, there were no significant relationships between the edge density of structural diversity or an interaction with forest type with  $\text{NDVI}$ . Forest type and longitude had the strongest significant relationships with  $\text{NDVI}$ , respectively, across all  $\text{GSM-SD}$ . Latitude had a weaker correlation of  $\text{NDVI}$  in three models (Sq  $\text{CHM}$  and  $\text{Q25}$ , Sbi  $\text{CV(ht)}$ ). Individual site-level regressions of  $\text{GSM-SD}$  that were correlated with  $\text{NDVI}$  exhibited many insignificant site-level regressions, but there were several significant site-level positive and negative relationships of  $\text{GSM-SD}$  and  $\text{NDVI}$  (Appendix S2: Table S1).

## DISCUSSION

We generated  $\text{GSM-SD}$  reflecting the landscape heterogeneity, dominance, and edge density of structural diversity across macrosystems and found that they varied by several environmental factors and were negatively correlated with productivity. First, the landscape composition and configuration of structural diversity as measured by  $\text{GSMs}$  often varied by factors that are indicative of or commonly responsible for environmental heterogeneity across macrosystems—forest type, geographic location, and climate—indicating that environmental and biological factors may influence the spatial patterns of structural

**TABLE 4** Macroscale variables that are related to GSM-SD: Forest type, geographic location, and climate.

Structural diversity	GSM	Forest type	Latitude	Longitude	Temperature	Precipitation
df		2	1	1	1	1
CHM	Sq	<b>12.478</b> ( <b>0.029, 0.133</b> )	<b>9.310</b> ( <b>0.029, 0.133</b> )	<b>8.286</b> ( <b>-0.129, -0.024</b> )	<b>74.909</b> ( <b>0.174, 0.276</b> )	<b>108.64</b> ( <b>0.218, 0.319</b> )
	Sbi	<b>27.368</b> (-0.063, 0.040)	0.185 (-0.063, 0.040)	<b>9.265</b> ( <b>0.028, 0.133</b> )	<b>3.964</b> ( <b>0.000, 0.105</b> )	<b>10.925</b> ( <b>-0.140, -0.035</b> )
	Sdr	4.341 (-0.070, 0.034)	0.456 (-0.070, 0.034)	<b>7.604</b> ( <b>0.021, 0.125</b> )	<b>6.715</b> ( <b>0.016, 0.121</b> )	<b>10.233</b> ( <b>0.033, 0.137</b> )
Q25	Sq	<b>124.95</b> ( <b>0.191, 0.292</b> )	<b>86.956</b> ( <b>0.191, 0.292</b> )	<b>37.047</b> ( <b>-0.212, -0.108</b> )	<b>37.681</b> ( <b>0.110, 0.213</b> )	<b>74.045</b> ( <b>0.173, 0.275</b> )
	Sbi	<b>4.032</b> (-0.011, 0.093)	2.384 (-0.011, 0.093)	0.521 (-0.071, 0.033)	<b>23.934</b> ( <b>0.077, 0.181</b> )	3.139 (-0.005, 0.099)
	Sdr	0.022 (-0.069, 0.035)	0.413 (-0.069, 0.035)	1.642 (-0.018, 0.086)	<b>7.251</b> ( <b>0.019, 0.124</b> )	<b>10.328</b> ( <b>0.033, 0.137</b> )
VCI	Sq	4.521 (-0.014, 0.090)	1.994 (-0.014, 0.090)	0.034 (-0.047, 0.057)	3.227 (-0.004, 0.100)	0.926 (-0.078, 0.026)
	Sbi	3.780 (-0.036, 0.067)	0.334 (-0.036, 0.067)	0.158 (-0.063, 0.041)	0.021 (-0.048, 0.056)	<b>22.456</b> ( <b>-0.177, -0.073</b> )
	Sdr	4.066 (-0.035, 0.069)	0.422 (-0.035, 0.069)	0.301 (-0.037, 0.067)	2.218 (-0.0125, 0.092)	5.033 (-0.007, 0.112)
CV(ht)	Sq	<b>17.712</b> ( <b>0.048, 0.153</b> )	<b>14.438</b> ( <b>0.048, 0.153</b> )	2.105 (-0.013, 0.091)	<b>4.166</b> ( <b>0.002, 0.106</b> )	2.493 (-0.010, 0.094)
	Sbi	<b>154.25</b> ( <b>0.193, 0.295</b> )	<b>88.962</b> ( <b>0.193, 0.295</b> )	<b>25.49</b> ( <b>-0.185, -0.081</b> )	0.256 (-0.038, 0.065)	1.042 (-0.079, 0.025)
	Sdr	2.664 (-0.093, 0.011)	2.389 (-0.093, 0.011)	0.168 (-0.041, 0.063)	<b>6.678</b> ( <b>0.016, 0.121</b> )	3.562 (-0.001, 0.102)

*Note:* A significant relationship in each univariate GLM is shown as a  $\chi^2$  statistic in boldface. Variables were natural  $\log(1 + x)$  transformed and then standardized to show effect size. The bootstrapped coefficients are shown to demonstrate the magnitude and direction of their relationships for the continuous variables, while differences in the mean and distribution of GSM-SD by forest type can be found in Figure 1.

diversity in predictable ways. Second, we found that dominance and heterogeneity GSM-SD were negatively related to ecosystem productivity (NDVI) across macrosystems, but these relationships were moderated by forest type. This study is a first step to applying a landscape gradient surface approach to quantifying the landscape composition and configuration of a new aspect of biological diversity (structural diversity) with GSMS and their potential value for understanding spatial relationships of structural diversity with ecosystem function across macrosystems.

## Macrosystem patterns of spatial variation in GSM-SD

Macrosystems are environmentally heterogeneous (Dodonov & Harper, 2022; Kane et al., 2011) and biological factors such as species composition and ecosystem identity (Turner, 1990, 2010; Turner & Gardner, 2015) can influence spatial patterns observed within macrosystems,

which was reflected by our finding that GSM-SD often differed by forest type. Structural diversity has been shown to vary considerably at small footprints and across ecotones (Atkins et al., 2022; Fotis et al., 2018; Hardiman et al., 2018). We found that evergreen, mixed, or deciduous forests had differences in their heterogeneity and dominance GSM-SD but not edge density. The landscape patterns of structural diversity may differ by forest type because they have different species compositions that exhibit different plant architecture (e.g., conical evergreen versus wide canopy deciduous forests) (Fang et al., 2017). Furthermore, differences in the competition for light and other resources between evergreen, mixed, and deciduous forests based on differences in species architecture and functional traits may also influence spatial patterns (McNeil et al., 2023), such as the dominance or heterogeneity of structural diversity.

Past work has shown that structural diversity correlates with macroscale climate patterns (Ehbrecht et al., 2021; LaRue, Knott, et al., 2023), so we expect that

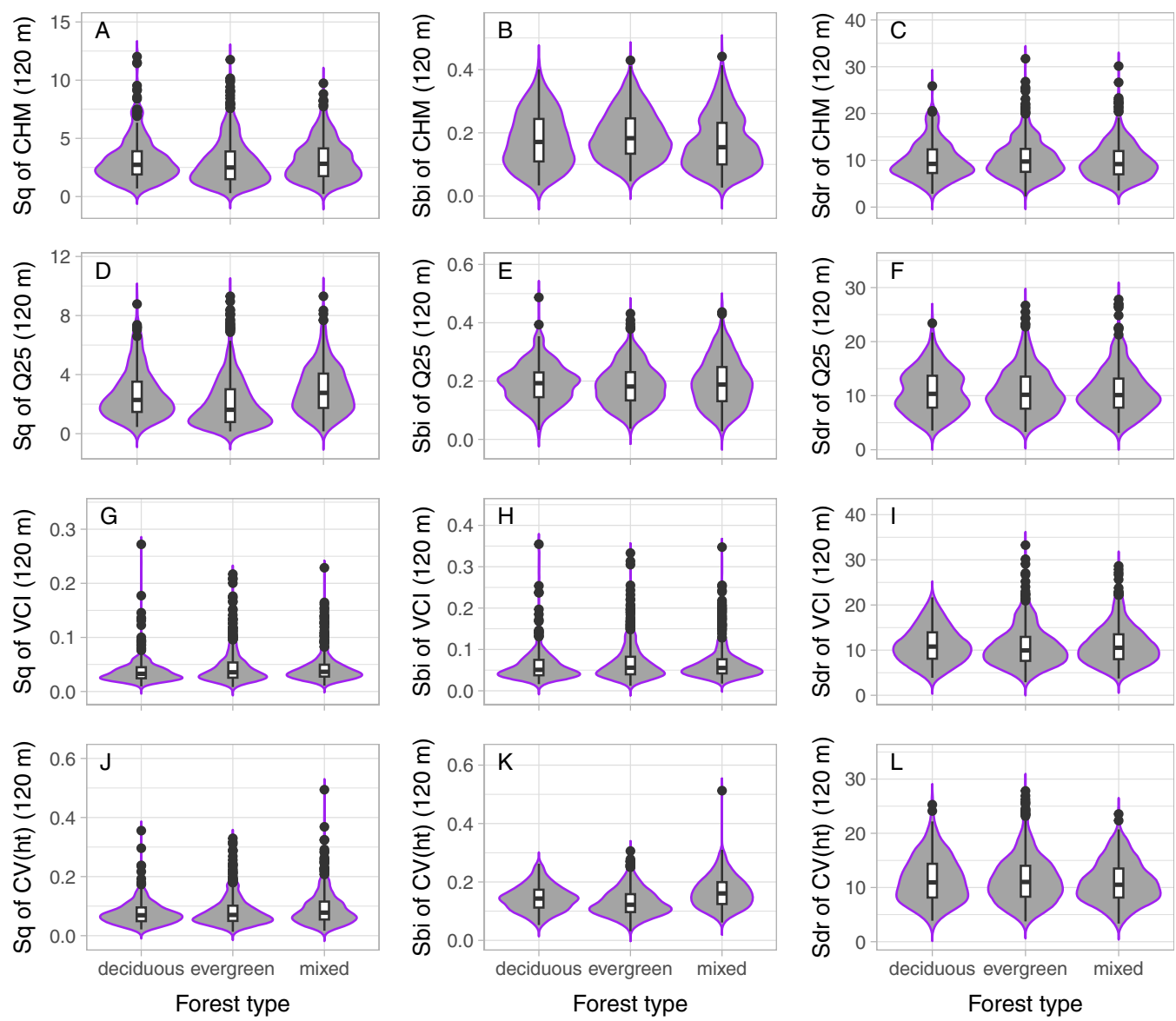


**FIGURE 2** Distribution of GSMS of structural diversity (GSM-SD) values within  $120 \times 120$  m patches at 28 NEON sites (absolute values shown) by forest type. Metric definitions for gradient surface metrics (GSMS) and structural diversity metrics can be found in Tables 1 and 3, respectively.

climate, and geographic location, would also show associations with the landscape composition and configuration of structural diversity. A productive or older ecosystem found in warm, wet climates will have more plant species, large individuals, and those of different sizes that should create spatial heterogeneity of structural diversity on the landscape (Franklin & Van Pelt, 2004; Kane et al., 2011). Therefore, GSM-SD that reflect heterogeneity or edge density may increase with higher temperature and precipitation (i.e., corresponding to lower latitude and higher longitude). Indeed, geographic location and climate were significantly related to several GSM-SD across macrosystems in our study. Several heterogeneity and edge density GSM-SD increased with precipitation,

while dominance GSMS decreased with precipitation; this was consistent with a macroscale pattern of decreases in heterogeneity and increases in dominance of peaks in canopy height values toward the arid Western United States. We saw GSM-SD that were positively associated with both temperature and latitude. While the positive relationships with temperature are consistent with the expectation that warmer, productive ecosystems will exhibit more landscape heterogeneity or edges in structural diversity, the positive relationship with latitude was counter to this and may indicate another factor such as disturbance or specific land use changes that increase GSM-SD with latitude. Our study is a first step toward understanding the complex set of factors that shape the

**TABLE 5** Relationship between GSM-SD with NDVI across macrosystems.

Structural diversity	GSM	GSM-SD (coefficient)	Forest type	Latitude	Longitude	GSM-SD × forest type
df		1		2	1	2
CHM	Sq	1.34 (−0.143, 0.036)	<b>491.35</b>	<b>5.52</b>	<b>177.76</b>	<b>97.21</b>
	Sbi	<b>29.53 (−0.325, −0.152)</b>	<b>452.63</b>	0.56	<b>153.98</b>	<b>31.07</b>
	Sdr	3.14 (−0.170, 0.008)	<b>444.04</b>	0.19	<b>167.98</b>	3.24
Q25	Sq	1.23 (−0.043, 0.158)	<b>446.18</b>	<b>10.43</b>	<b>146.32</b>	<b>46.65</b>
	Sbi	<b>10.97 (−0.261, −0.067)</b>	<b>488.34</b>	1.82	<b>155.95</b>	<b>87.26</b>
	Sdr	0.51 (−0.058, 0.126)	<b>443.30</b>	0.14	<b>170.42</b>	4.28
VCI	Sq	<b>8.68 (−0.231, −0.046)</b>	<b>458.02</b>	0.66	<b>165.28</b>	<b>36.08</b>
	Sbi	<b>13.75 (−0.271, −0.083)</b>	<b>449.43</b>	0.32	<b>159.56</b>	<b>24.88</b>
	Sdr	0.11 (−0.110, 0.078)	<b>432.40</b>	0.01	<b>175.90</b>	4.20
CV(ht)	Sq	<b>4.86 (−0.224, −0.013)</b>	<b>456.63</b>	1.41	<b>183.73</b>	<b>74.37</b>
	Sbi	2.24 (−0.183, 0.024)	<b>430.65</b>	<b>4.79</b>	<b>146.64</b>	<b>47.93</b>
	Sdr	0.40 (−0.061, 0.120)	<b>439.79</b>	0.05	<b>171.04</b>	0.49

*Note:* A significant correlation in the GLM model, NDVI ~ GSM-SD + forest type + GSM-SD × forest type + latitude + longitude, is shown as a  $\chi^2$  statistic in boldface. Variables were natural log(1 + x) transformed and then standardized to show effect size ( $N_{\text{Patches}} = 1400$ ). The bootstrapped coefficient of GSM-SD is shown to demonstrate the magnitude and direction of their relationship with NDVI.

landscape composition and configuration of structural diversity across macrosystems, but future work should continue to investigate the influence of a suite of disturbance and other biotic drivers that were beyond the scope of this study.

## GSM-SD as a correlate of forest productivity across macrosystems

Our study results were consistent with the expectation that there will be a negative relationship between the patch heterogeneity of structural diversity and productivity. Structural diversity is thought to enhance ecosystem function (Aponte et al., 2020; Gough et al., 2019; LaRue, Knott, et al., 2023) through the filling of plants in different vertical niche space (Hardiman et al., 2011; LaRue, Knott, et al., 2023; Niinemets, 2010). Therefore, for high heterogeneity of structural diversity within the same patch (i.e., departure from the mean), we expected that this could lead to a reduction in productivity due to a breakup of the filling of vertical niche space in the canopy across space. Indeed, patch-level heterogeneity in structural diversity had a negative relationship with NDVI across macrosystems. This relationship with heterogeneity GSM-SD and productivity was moderated by forest type with evergreen forested sites trending toward a positive and deciduous or mixed forest a negative relationship with NDVI. At the site level, evergreen forests also had most of the positive relationships (e.g., ABBY, NIWO, and RMNP) and deciduous forests negative with

NDVI (SERC, UKFS, and LENO). The crown shape of evergreen tree species may allow for differential light capture and canopy packing at the patch level (Horn, 1971; McNeil et al., 2023) such that there was a benefit of landscape heterogeneity in structural diversity for resource uptake in evergreen forests at the size of the patches we measured. However, larger patches may or may not see a consistently negatively relationship due to cross-scale interactions that moderate the relationships between heterogeneity in structural diversity and productivity. It was beyond the scope of this study, but scale, species composition, or disturbance history may play a critical role in shaping the landscape heterogeneity of structural diversity (Atkins et al., 2020; Choi et al., 2023), and thereby its consequences on ecosystem function.

A landscape that has a dominance in many high peaks of structural diversity values should be negatively related to ecosystem functions like productivity due to a predominance of high peaks of values rather than a more evenly peaked area (LaRue, Knott, et al., 2023). This hypothesis was supported for three structural diversity metrics in height and vertical complexity in our study such that a higher patch-level dominance of high peaks in structural diversity (as opposed to a more evenly distributed patch with few high peaks) was negatively related to productivity across macrosystems. Additionally, we saw differences in the direction of the relationship by forest type with positive correlations for evergreen and negative for deciduous or mixed for canopy height and vertical complexity index (VCI). This opposing relationship by forest type may have occurred due to differential competition

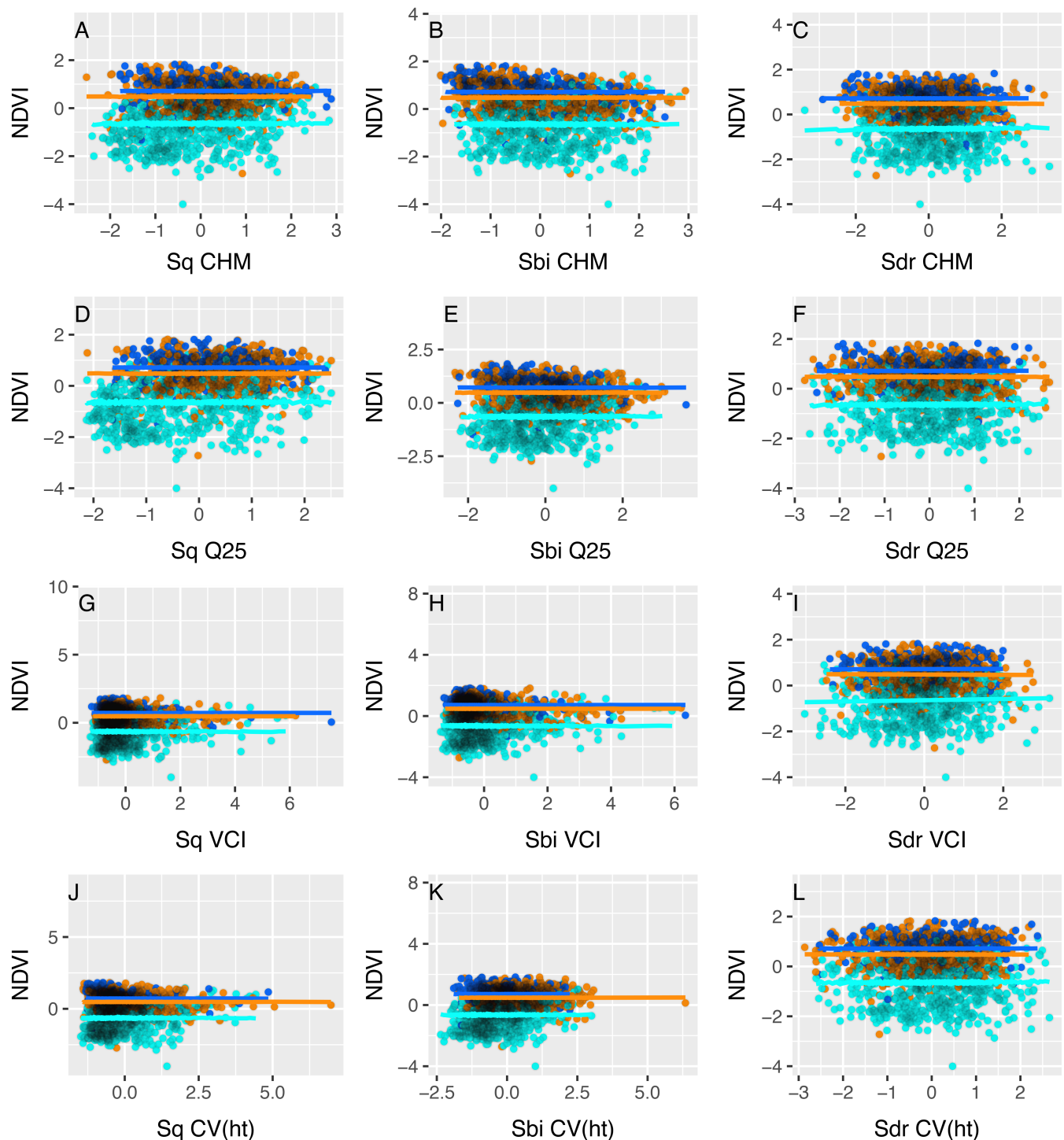


**FIGURE 3** Relationship between GSM-SD and NDVI by forest type across macrosystems. Corresponding model results can be found in Table 5. The trend line shows the interaction between the GSM-SD and forest type. Variables were natural  $\log(1 + x)$  transformed and standardized for effect size. Metric definitions for GSMS and structural diversity metrics can be found in Tables 1 and 3, respectively. Line colors indicate forest type: blue, deciduous; orange, mixed; turquoise, evergreen.

between evergreen versus deciduous tree species (Álvarez-Yépez et al., 2017; Givnish, 2002; Sprugel, 1989). In general, dominance GSMS (i.e., Sbi) therefore appear to represent useful metrics for quantifying patch-level dominance in high peak values of structural diversity related to

ecosystem function, but there are GSMS that describe other aspects of landscape dominance or evenness patterns that may shed additional light on the landscape patterns of structural diversity (see McGarigal et al., 2009). For example, future work could investigate the minima and

maxima of structural diversity values that would indicate the location of old growth patches that represent the ideal breeding habitat for the endangered Mexican spotted owl (Durboraw et al., 2022; Witt et al., 2022) and other threatened wildlife.

Over macrosystems, we saw forest and site variation in the edge density of structural diversity but no relationship with productivity. We predicted that a landscape that had patches with high edge density of structural diversity may be negatively correlated with forest productivity due to two potential mechanisms. First, a landscape with many edges in its structural diversity metric (deviations from the mean) could provide reductions in productivity as it would detract from the filling of vertical niche space at different points within the patch (LaRue, Knott, et al., 2023). Second, a greater edge density may mark a transition in structural attributes that represent an ecotone or successional transition that may not promote productivity (Fahey et al., 2019). Conventional knowledge is that forest edges negatively influence forest structure and thereby carbon as seen in the tropics (Chaplin-Kramer et al., 2015; Ordway & Asner, 2020), but here, there was no measurable relationship with the ecosystem function of productivity when edge density of structural diversity was high or low. However, work in temperature forests observed elevated growth along forest edges (Morreale et al., 2021). Edge density of structural diversity across different forest types and regions might have variable relationships to productivity or previous work may have focused on abrupt forest edges that has different a relationship with GSM-SD of edge density in forested areas (i.e., we did not look at edges between forest and other land cover types) and productivity across the landscape in our study.

## Conclusion

Structural diversity can now be more readily measured by remote-sensing tools across macrosystems (Fahey et al., 2018; LaRue, Fahey, et al., 2023; Valbuena et al., 2020) compared with the period of conceptualization in the early 20th century (i.e., MacArthur & MacArthur, 1961). Metrics derived from remote sensing that describe the landscape composition and configuration of structural diversity may therefore provide useful for managing ecosystem function (LaRue, Fahey, et al., 2023). We demonstrate the effectiveness of employing GSMS as a method to quantify the landscape composition and configuration of a novel aspect of diversity. The GSM-SD exhibited variation through different forest types, climate, and geographic location across macrosystems, and landscape patterns of dominance and

heterogeneity, but not edge density, in structural diversity were found to be linked to ecosystem productivity. The utility of applying the patch mosaic paradigm to a continuous 3D diversity variable across landscapes and macrosystems may allow for a better understanding of the environmental drivers and impacts to ecosystem functions and in spatially motivated management decisions.

## AUTHOR CONTRIBUTIONS

Elizabeth A. LaRue conceptualized the idea through discussions with Songlin Fei and Brady S. Hardiman. Elizabeth A. LaRue, Kylie M. Rezendes, Anna G. Downing, Jianmin Wang, and Dennis H. Choi conducted the spatial data processing and Elizabeth A. LaRue conducted the statistical analyses. Elizabeth A. LaRue led the writing with all authors contributing. Elizabeth A. LaRue, Songlin Fei, and Brady S. Hardiman secured the funding.

## ACKNOWLEDGMENTS

Funding for this work was supported by the GEO-Microsoft Planetary Computer Credits Programme and NSF DEB number 2212859 to EAL, NSF DEB number 1926538 to BSH, and NSF DEB number 2106103 to SF and EAL, and NIFA grant number 2023-68012-38992 and number 2024-67021-42879 to SF and BSH. We thank A. Benson for help with obtaining Landsat data and for the anonymous reviewer feedback.

## CONFLICT OF INTEREST STATEMENT

The authors declare no conflicts of interest.

## DATA AVAILABILITY STATEMENT

Data used are available as follows: Structural diversity derived from NEON AOP Lidar are found on the Environmental Data Initiative (Wang et al., 2023, 2024), Landsat 8 Collection 2-Level from the USGS Earth Explorer (<https://earthexplorer.usgs.gov>) and from the Microsoft Planetary Computer ([www.planetarycomputer.microsoft.com](http://www.planetarycomputer.microsoft.com)) as described in Methods, and land cover from the ESRI Living Atlas, 2019 (<https://livingatlas.arcgis.com/landcover/>). Analysis code and the derived data in .csv format (LaRue et al., 2025) are available from Zenodo: <https://doi.org/10.5281/zenodo.14617612>.

## ORCID

Elizabeth A. LaRue  <https://orcid.org/0000-0002-9535-0630>

Kylie M. Rezendes  <https://orcid.org/0009-0003-3803-1144>

Dennis H. Choi  <https://orcid.org/0000-0002-4038-9204>

Jianmin Wang  <https://orcid.org/0000-0001-6739-9499>

Anna G. Downing  <https://orcid.org/0000-0001-7654-7342>  
 Songlin Fei  <https://orcid.org/0000-0003-2772-0166>  
 Brady S. Hardiman  <https://orcid.org/0000-0001-6833-9404>

## REFERENCES

Álvarez-Yépez, J. C., A. Búrquez, A. Martínez-Yrízar, M. Teece, E. A. Yépez, and M. Dovciak. 2017. "Resource Partitioning by Evergreen and Deciduous Species in a Tropical Dry Forest." *Oecologia* 183: 607–618.

Anderson, M. G., P. J. Comer, P. Beier, J. J. Lawler, C. A. Schloss, S. Buttrick, C. M. Albano, and D. P. Faith. 2015. "Case Studies of Conservation Plans That Incorporate Geodiversity." *Conservation Biology* 29: 680–691.

Aponte, C., S. Kasel, C. R. Nitschke, M. A. Tanase, H. Vickers, L. Parker, M. Fedrigo, et al. 2020. "Structural Diversity Underpins Carbon Storage in Australian Temperate Forests." *Global Ecology and Biogeography* 29: 789–802.

Atkins, J. W., B. Bond-Lamberty, R. T. Fahey, L. T. Haber, E. Stuart-Haëntjens, B. S. Hardiman, E. LaRue, et al. 2020. "Application of Multidimensional Structural Characterization to Detect and Describe Moderate Forest Disturbance." *Ecosphere* 11: e03156.

Atkins, J. W., J. Costanza, K. M. Dahlin, M. P. Dannenberg, A. J. Elmore, M. C. Fitzpatrick, C. R. Hakkenberg, et al. 2023. "Scale Dependency of Lidar-Derived Forest Structural Diversity." *Methods in Ecology and Evolution* 14: 708–723.

Atkins, J. W., R. T. Fahey, B. H. Hardiman, and C. M. Gough. 2018. "Forest Canopy Structural Complexity and Light Absorption Relationships at the Subcontinental Scale." *Journal of Geophysical Research: Biogeosciences* 123: 1387–1405.

Atkins, J. W., J. A. Walter, A. E. L. Stovall, R. T. Fahey, and C. M. Gough. 2022. "Power Law Scaling Relationships Link Canopy Structural Complexity and Height across Forest Types." *Functional Ecology* 36: 713–726.

Biband, R., T. Keitt, and B. Rowlingson. 2022. "rgdal: Bindings for the 'Geospatial' Data Abstraction Library." R Version 1.5–32. <https://proj.org>, <https://r-forge.r-project.org/projects/rgdal/>.

Brodie, J. F., and P. D. Mannion. 2023. "The Hierarchy of Factors Predicting the Latitudinal Diversity Gradient." *Trends in Ecology & Evolution* 38: 15–23.

Chaplin-Kramer, R., I. Ramler, R. Sharp, N. M. Haddad, J. S. Gerber, P. C. West, L. Mandle, et al. 2015. "Degradation in Carbon Stocks near Tropical Forest Edges." *Nature Communications* 6: 10158.

Choi, D. H., E. A. LaRue, J. W. Atkins, J. R. Foster, J. H. Matthes, R. T. Fahey, B. Thapa, S. Fei, and B. S. Hardiman. 2023. "Short-Term Effects of Moderate Severity Disturbances on Forest Canopy Structure." *Journal of Ecology* 111: 1866–81.

Crockett, E. T. H., J. W. Atkins, Q. Guo, G. Sun, K. M. Potter, S. Ollinger, C. A. Silva, et al. 2023. "Structural and Species Diversity Explain Aboveground Carbon Storage in Forests across the United States: Evidence from GEDI and Forest Inventory Data." *Remote Sensing of Environment* 295: 113703.

Dodonov, P., and K. Harper. 2022. "Spatial Patterns of Structural Diversity Across the Boreal Forest-Tundra Ecotone in Churchill, Canada." *Acta Oecologica* 117: 103862.

Durboraw, T. D., C. W. Boal, M. S. Fleck, and N. S. Gill. 2022. "Long-Term Recovery of Mexican Spotted Owl Nesting Habitat after Fire in the Lincoln National Forest, New Mexico." *Fire Ecology* 18: 31.

Ehbrecht, M., D. Seidel, P. Annighöfer, H. Kreft, M. Köhler, D. C. Zemp, K. Puettmann, et al. 2021. "Global Patterns and Climatic Controls of Forest Structural Complexity." *Nature Communications* 12: 1–12.

ESRI Living Atlas. 2019. "Sentinel-2 10-Meter Land Use/Land Cover." <https://earthexplorer.usgs.gov>.

Fahey, R. T., B. C. Alveshere, J. I. Burton, A. W. D'Amato, Y. L. Dickinson, W. S. Keeton, C. C. Kern, et al. 2018. "Shifting Conceptions of Complexity in Forest Management and Silviculture." *Forest Ecology and Management* 421: 59–71.

Fahey, R. T., J. W. Atkins, C. M. Gough, B. S. Hardiman, L. E. Nave, J. M. Tallant, K. J. Nadehoffer, et al. 2019. "Defining a Spectrum of Integrative Trait-Based Vegetation Canopy Structural Types." *Ecology Letters* 22: 2049–59.

Fang, X., G. Shen, Q. Yang, H. Liu, Z. Ma, D. C. Deane, and X. Wang. 2017. "Habitat Heterogeneity Explains Mosaics of Evergreen and Deciduous Trees at Local-Scales in a Subtropical Evergreen Broad-Leaved Forest." *Journal of Vegetation Science* 28: 379–388.

Fei, S., Q. Guo, and K. Potter. 2016. "Macrosystems Ecology: Novel Methods and New Understanding of Multi-Scale Patterns and Processes." *Landscape Ecology* 31: 1–6.

Fotis, A. T., T. H. Morin, R. T. Fahey, B. S. Hardiman, G. Bohrer, and P. S. Curtis. 2018. "Forest Structure in Space and Time: Biotic and Abiotic Determinants of Canopy Complexity and their Effects on Net Primary Productivity." *Agricultural and Forest Meteorology* 250: 181–191.

Franklin, J., and R. Van Pelt. 2004. "Spatial Aspects of Structural Complexity in Old-Growth Forests." *Journal of Forestry* 102: 22–28.

Gaston, K., P. Williams, P. Eggleton, and C. Humphries. 1995. "Large Scale Patterns of Biodiversity: Spatial Variation in Family Richness." *Proceedings of the Royal Society of London. Series B: Biological Sciences* 260: 149–154.

Givnish, T. J. 2002. "Adaptive Significance of Evergreen vs. Deciduous Leaves: Solving the Triple Paradox." *Silva Fennica* 36: 703–743.

Gough, C. M., J. W. Atkins, R. T. Fahey, and B. S. Hardiman. 2019. "High Rates of Primary Production in Structurally Complex Forests." *Ecology* 100: 1–6.

Guo, Q., A. Chen, E. T. H. Crockett, J. W. Atkins, X. Chen, and S. Fei. 2023. "Integrating Gradient with Scale in Ecological and Evolutionary Studies." *Ecology* 104: e3982.

Hardiman, B. S., G. Bohrer, C. M. Gough, C. S. Vogel, and P. S. Curtis. 2011. "The Role of Canopy Structural Complexity in Wood Net Primary Production of a Maturing Northern Deciduous Forest." *Ecology* 92: 1818–27.

Hardiman, B. S., E. A. LaRue, J. W. Atkins, R. T. Fahey, F. W. Wagner, and C. M. Gough. 2018. "Spatial Variation in Canopy Structure across Forest Landscapes." *Forests* 9: 474.

Hawkins, B., E. Porter, and J. Felizola Diniz-Filho. 2003. "Productivity and History as Predictors of the Latitudinal Diversity Gradient of Terrestrial Birds." *Ecology* 84: 1608–23.

Hijmans, R. 2024. "terra: Spatial Data Analysis." R Package Version 1.7–46. <https://rspatial.github.io/terra/>, <https://rspatial.org/>.

Hijmans, R., and J. van Etten. 2022. "raster: Geographic Analysis and Modeling with Raster Data." R Package Version 3.6-3. <http://CRAN.R-project.org/package=raster>.

Horn, H. S. 1971. *The Adaptive Geometry of Trees*. Princeton, NJ: Princeton University Press.

Kane, V., R. Gersonde, J. Lutz, R. McGaughey, J. Bakker, and J. Franklin. 2011. "Patch Dynamics and the Development of Structural and Spatial Heterogeneity in Pacific Northwest Forests." *Canadian Journal of Forestry* 2011: 2276–91.

Kedron, P., Y. Zhao, and A. E. Frazier. 2019. "Three Dimensional (3D) Spatial Metrics for Objects." *Landscape Ecology* 34: 2123–32.

LaRue, E., J. Knott, G. Domke, H. Chen, Q. Guo, M. Hisano, C. Oswalt, et al. 2023. "Structural Diversity as a Reliable and Novel Predictor for Ecosystem Productivity." *Frontiers in Ecology and the Environment* 21: 33–39.

LaRue, E., K. Rezendes, D. H. Choi, J. Wang, A. Downing, S. Fei, and B. Hardiman. 2025. "Gradient Surface Metrics of Ecosystem Structural Diversity and their Relationship with Productivity across Macrosystems." Zenodo. <https://doi.org/10.5281/zenodo.14617611>.

LaRue, E. A., R. Fahey, B. Alveshere, J. W. Atkins, B. Buma, A. Chen, S. Cousins, et al. 2023. "A Framework for the Ecological Role of Structural Diversity." *Frontiers in Ecology and the Environment* 21: 4–13.

MacArthur, R. H., and J. W. MacArthur. 1961. "On Bird Species Diversity." *Ecology* 42: 594–98.

McGarigal, K., and S. Dushman. 2005. "The Gradient Concept of Landscape Structure." In *Issues and Perspectives in Landscape Ecology*, edited by J. Wiens and M. Moss, 112–19. Cambridge: Cambridge University Press.

McGarigal, K., and B. A. Marks. 1995. "FRAGSTATS v2: Spatial Pattern Analysis Program for Quantifying Landscape Structure." Computer Software Program Produced by the Authors at the University of Massachusetts, Amherst. <http://www.umass.edu/landeco/research/f>.

McGarigal, K., S. Tagil, and S. A. Cushman. 2009. "Surface Metrics: An Alternative to Patch Metrics for the Quantification of Landscape Structure." *Landscape Ecology* 24: 433–450.

McNeil, B., R. Fahey, C. King, D. Erazo, T. Z. Heimerl, and A. Elmore. 2023. "Tree Crown Economics." *Frontiers in Ecology and the Environment* 21: 40–48.

Morreale, L. L., J. R. Thompson, X. Tang, A. B. Reinmann, and L. R. Hutyra. 2021. "Elevated Growth and Biomass along Temperate Forest Edges." *Nature Communications* 12: 7181.

Myineni, R. B., F. G. Hall, P. J. Sellers, and A. L. Marshak. 1995. "The Interpretation of Spectral Vegetation Indexes." *IEEE Transactions on Geoscience and Remote Sensing* 33: 481–86.

NEON. 2025. Discrete Return LiDAR Point Cloud (DP1.30003.001). <https://data.neonscience.org/data-products/DP1.30003.001>.

Niinemets, Ü. 2010. "A Review of Light Interception in Plant Stands from Leaf to Canopy in Different Plant Functional Types and in Species with Varying Shade Tolerance." *Ecological Research* 25: 693–714.

Ogunjemiyo, S., G. Parker, and D. Roberts. 2005. "Reflections in Bumpy Terrain: Implications of Canopy Surface Variations for the Radiation Balance of Vegetation." *IEEE Geoscience and Remote Sensing Letters* 2: 90–93.

Ordway, E. M., and G. P. Asner. 2020. "Carbon Declines along Tropical Forest Edges Correspond to Heterogeneous Effects on Canopy Structure and Function." *Proceedings of the National Academy of Sciences of the United States of America* 117: 7863–70.

Pettorelli, N., J. O. Vik, A. Mysterud, J.-M. Gaillard, C. J. Tucker, and N. C. Stenseth. 2005. "Using the Satellite-Derived NDVI to Assess Ecological Responses to Environmental Change." *Trends in Ecology & Evolution* 20: 503–510.

Read, Q. D., P. L. Zarnetske, S. Record, K. M. Dahlin, J. K. Costanza, A. O. Finley, K. D. Gaddis, et al. 2020. "Beyond Counts and Averages: Relating Geodiversity to Dimensions of Biodiversity." *Global Ecology and Biogeography* 29: 696–710.

Roussel, J.-R., D. Auty, N. C. Coops, P. Tompalski, T. R. H. Goodbody, A. S. Meador, J.-F. Bourdon, F. de Boissieu, and A. Achim. 2020. "lidR: An R Package for Analysis of Airborne Laser Scanning (ALS) Data." *Remote Sensing of Environment* 251: 112061.

Smith, A. C., K. M. Dahlin, S. Record, J. K. Costanza, A. M. Wilson, and P. L. Zarnetske. 2021. "The Geodiv R Package: Tools for Calculating Gradient Surface Metrics." *Methods in Ecology and Evolution* 12: 2094–2100.

Sprugel, D. 1989. "The Relationship of Evergreeness, Crown Architecture, and Leaf Size." *The American Naturalist* 133: 465–479.

Torresan, C., M. del Río, T. Hilmers, M. Notarangelo, K. Bielak, F. Binder, A. Boncina, et al. 2020. "Importance of Tree Species Size Dominance and Heterogeneity on the Productivity of Spruce-Fir-Beech Mountain Forest Stands in Europe." *Forest Ecology and Management* 457: 117716.

Tscharntke, T., J. M. Tylianakis, T. A. Rand, R. K. Didham, L. Fahrig, P. Batáry, J. Bengtsson, et al. 2012. "Landscape Moderation of Biodiversity Patterns and Processes - Eight Hypotheses." *Biological Reviews* 87: 661–685.

Turner, M., and R. Gardner. 2015. *Landscape Ecology in Theory and Practice: Pattern and Process*, Second ed. New York: Springer.

Turner, M. G. 1990. "Spatial and Temporal Analysis of Landscape Patterns." *Landscape Ecology* 4: 21–30.

Turner, M. G. 2010. "Disturbance and Landscape Dynamics in a Changing World." *Ecology* 91: 2833–49.

U.S. Geological Survey. 2023. "Landsat 8." Archived by National Aeronautics and Space Administration, U.S. Government, U.S. Geological Survey, Sioux Falls, South Dakota, USA.

Valbuena, R., B. O'Connor, F. Zellweger, W. Simonson, P. Vihervaara, M. Maltamo, C. A. Silva, et al. 2020. "Standardizing Ecosystem Morphological Traits from 3D Information Sources." *Trends in Ecology and Evolution* 35: 656–667.

van Ewijk, K. Y., P. M. Treitz, and N. A. Scott. 2011. "Characterizing Forest Succession in Central Ontario Using Lidar-Derived Indices." *Photogrammetric Engineering & Remote Sensing* 77: 261–69.

Wang, J., D. Choi, E. LaRue, J. Atkins, J. Foster, J. Matthes Hatala, R. Fahey, S. Fei, and B. Hardiman. 2023. "Structural Diversity from the NEON Discrete-Return LiDAR Point Cloud in 2013–2022." *Environmental Data Initiative*. <https://doi.org/10.6073/pasta/e02f855d69193a46571168575b35291d>.

Wang, J., D. H. Choi, E. LaRue, J. W. Atkins, J. R. Foster, J. H. Matthes, R. T. Fahey, S. Fei, and B. S. Hardiman. 2024. "NEON-SD: A 30-m Structural Diversity Product Derived from the NEON Discrete-Return LiDAR Point Cloud." *Scientific Data* 11: 1174.

Witt, C., R. J. Davis, Z. Yang, J. L. Ganey, R. J. Gutiérrez, S. Healey, S. Hedwall, et al. 2022. "Linking Robust Spatiotemporal Datasets to Assess and Monitor Habitat Attributes of a Threatened Species." *PLoS One* 17: e0265175.

Zhang, J., C. Liu, Z. Ge, and Z. Zhang. 2024. "Stand Spatial Structure and Productivity Based on Random Structural Unit in *Larix principis-rupprechtii* Forests." *Ecosphere* 15(4): 4824.

Zimble, D. A., D. L. Evans, G. C. Carlson, R. C. Parker, S. C. Grado, and P. D. Gerard. 2003. "Characterizing Vertical Forest Structure Using Small-Footprint Airborne LiDAR." *Remote Sensing of Environment* 87: 171–182.

## SUPPORTING INFORMATION

Additional supporting information can be found online in the Supporting Information section at the end of this article.

**How to cite this article:** LaRue, Elizabeth A., Kylie M. Rezendes, Dennis H. Choi, Jianmin Wang, Anna G. Downing, Songlin Fei, and Brady S. Hardiman. 2025. "Gradient Surface Metrics of Ecosystem Structural Diversity and Their Relationship with Productivity across Macrosystems." *Ecosphere* 16(2): e70172. <https://doi.org/10.1002/ecs2.70172>